



Extracting dynamic topography from river profiles and cosmogenic nuclide geochronology in the Middle Atlas and the High Plateaus of Morocco



Alvar Pastor^{a,*}, Julien Babault^a, Lewis A. Owen^b, Antonio Teixell^a, María-Luisa Arboleya^a

^a Departament de Geologia, Universitat Autònoma de Barcelona, E-08193 Bellaterra, Spain

^b Department of Geology, University of Cincinnati, Cincinnati, OH 45221, USA

ARTICLE INFO

Article history:

Received 23 September 2014

Received in revised form 20 May 2015

Accepted 2 June 2015

Available online 20 June 2015

Keywords:

Atlas Mountains

River profile

Knickpoint

Cosmogenic dating

Active tectonics

Dynamic topography

ABSTRACT

The Moulouya river system has intensely eroded the Arhbalou, Missouri, and Guercif Neogene foreland basins in northeastern Morocco, having changed from net aggradation during the Miocene–early Pliocene to net incision punctuated by alluvial fan deposition at late Pliocene or early Quaternary time. This region as a whole has experienced mantle-driven, surface uplift (dynamic topography) since the late Cenozoic, being locally affected by uplift due to crustal shortening and thickening of the Middle Atlas too. Knickpoints located along the major streams of the Moulouya fluvial network, appear on both the undeformed margins of the Missouri and Guercif foreland basins (High Plateaus), as well as along the thrust mountain front of the southern Middle Atlas, where they reach heights of 800–1000 m. 500–550 m of the knickpoint vertical incision might be explained by long-wavelength mantle-driven dynamic surface uplift, whereas the remaining 450–500 m in the southern Middle Atlas front and 200–300 m in the northeastern Middle Atlas front seem to be thrust-related uplift of the Jebel Bou Naceur. Be-10 terrestrial cosmogenic nuclides have been used to date two Quaternary river terraces in the Chegg Ard valley at 62 ± 14 ka and 411 ± 55 ka. The dated terraces allow the incision rates associated with the frontal structures of the Middle Atlas to be estimated at ~ 0.3 mm yr⁻¹. Furthermore, these ages have served to evaluate mantle-driven regional surface uplift since the middle Pleistocene in the central Missouri basin, yielding values of ~ 0.1 – 0.2 mm yr⁻¹.

© 2015 Elsevier B.V. All rights reserved.

1. Introduction

The Atlas Mountains of Morocco and the surrounding plains underwent long-wavelength surface uplift caused by thermal mantle-driven buoyancy since the late Cenozoic (Anahnah et al., 2011; Babault et al., 2008; Teixell et al., 2003, 2005; Zeyen et al., 2005). Deformation of drainage networks and geomorphic indexes suggest that surface uplift is still active (e.g., Barbero et al., 2011; Barcos et al., 2014). This mantle-driven surface uplift is superimposed onto the tectonic effect of the thickened crust of the High and Middle Atlas produced by thrusting since the Paleogene. Although tectonic shortening is moderate in the Atlas thrust belts, deformation registered in Quaternary alluvial deposits at the southern fronts of the High and Middle Atlas indicates that thrusting is still active (Delcaillau et al., 2008; Laville et al., 2007; Pastor et al., 2012; Sébrier et al., 2006). Within this framework, the landscape of the foreland of the High and Middle Atlas (Arhbalou, Missouri, and Guercif basins; Fig. 1), changed from net aggradation to erosion and fluvial incision in late Pliocene or Quaternary time (Bouazza et al.,

2009). The Moulouya river system currently drains these basins, its headwaters being located in the flanking reliefs of the Middle Atlas, the High Atlas, and the High Plateaus (Fig. 1a). The Arhbalou, Missouri, and Guercif basins are only deformed in the proximity of the High and Middle Atlas thrust fronts (Fig. 1b), and, together with the flanking mountain belts, provide a useful natural laboratory to examine the triggers of landscape change and, in particular, to evaluate the sources of surface uplift.

This work presents a tectonic and geomorphic study on the Arhbalou, Missouri and southern Guercif basins, as well as on their eastern and western margins, featuring an analysis of stream profiles in the upper Moulouya river drainage network. The river profiles reveal the systematic presence of large knickpoints or knickzones on tributaries draining both flanks of the Moulouya river system, i.e., the folded Middle Atlas and the undeformed High Plateaus, enabling a discussion on the origin of knickpoints as due to large-scale surface uplift. We present the first ¹⁰Be terrestrial cosmogenic nuclide (TCN) dating of Quaternary deposits within the Missouri basin, allowing the determination of fluvial incision rates since the Middle Pleistocene, which, in turn, can be converted to surface uplift rates. Combined with the geomorphic analysis, the geochronological data allow us to assess the relative role of different driving-mechanisms of surface uplift in the landscape evolution of the

* Corresponding author. Tel.: +34 569 93830679.

E-mail address: alvarpastorc@gmail.com (A. Pastor).

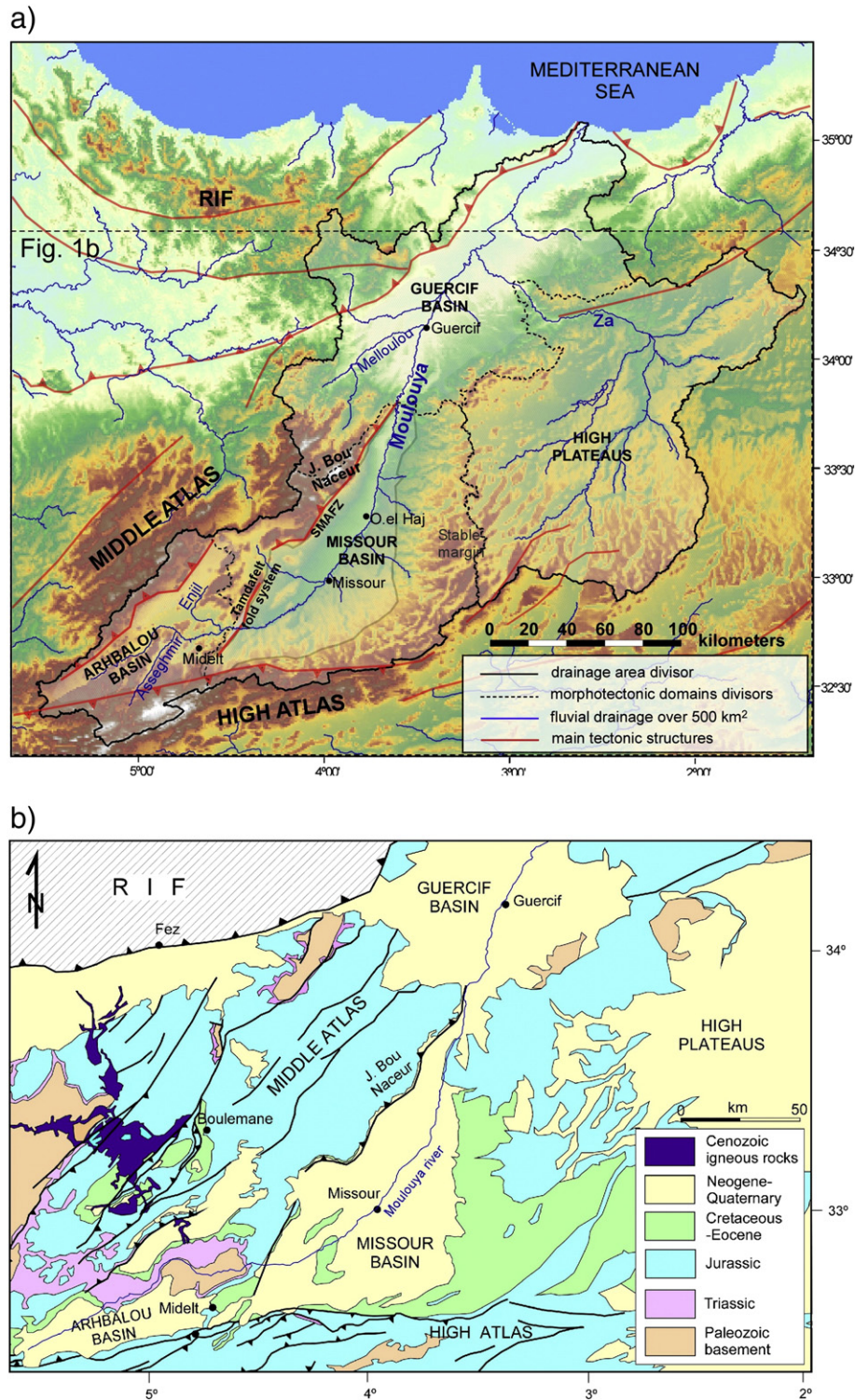


Fig. 1. a) Digital elevation model (DEM SRTM90) of northeastern Morocco, with the main morphotectonic features and the Moulouya drainage basin. SMAFZ, Southern Middle Atlas frontal zone. b) Geological map of part of the area shown in panel a.

northeastern Atlas region. Other studies elsewhere attempted to retrieve magnitudes of mantle-driven uplift from geomorphic indicators (e.g., Nereson et al., 2013; Paul et al., 2014; Schildgen et al., 2012). This study intends to discriminate for the first time the amount and rate of river incision directly related to tectonic deformation from those associated with the large-scale mantle-driven dynamic topography.

2. Regional setting

The Moulouya river (~650 km-long) is, after the Nile, the second largest river in North Africa that drains to the Mediterranean Sea (Fig. 1a). From headwaters to outlet, the Moulouya river flows across the Arhbalou, Missouri, and Guercif Neogene foreland basins, draining an area of ~74,000 km², that includes the High Plateaus in the east,

the High Atlas in the south, the Middle Atlas towards the west, and the eastern Rif in the north-west, to eventually enter the Mediterranean sea near Nador in northern Morocco. The Moulouya river begins at 2000 m.a.s.l. at the junction of the Middle and High Atlas, which is the drainage divide between rivers flowing to the Atlantic and to the Mediterranean. The course of the Moulouya river is at least twice the distance from its headwaters to the Atlantic. For that reason, slopes are steeper on the Atlantic Atlas side, where headward eroding rivers threaten to capture the upper part of the Moulouya catchment.

The geologic evolution of the Arhbalou and Missour sedimentary basins is related to the thrust loading of the Cenozoic High and Middle Atlas orogenic belts (Arboleya et al., 2004; Beauchamp et al., 1996), whereas the Guercif basin has been influenced by the Rif orogen (Gomez et al., 2000). These three basins are mostly filled with Miocene alluvial and lacustrine sediments. The sedimentary record has been described in detail by Bernini et al. (1999, 2000), Gomez et al. (2000), Krijgsman et al. (1999), Krijgsman and Langereis (2000) and Sani et al. (2000) for the Guercif basin, by Beauchamp et al. (1996) and Ellouz et al. (2003) for the Missour basin, and by Dutour (1983) for the Arhbalou basin. Bouazza et al. (2009) proposed that sedimentation in the Guercif basin ended at early Quaternary time when the basin probably have changed from endorheic to externally drained, connecting the Moulouya river to the Mediterranean Sea.

The Middle Atlas is a NE-trending, basement-involved thrust belt that derives from the inversion of a Triassic–Jurassic rift, with a relatively simple structure and a modest amount of total orogenic shortening (<10%, Gomez et al., 1998; Arboleya et al., 2004). The southern Middle Atlas front defines the western margin of the Missour basin (Fig. 1b). The mountain front coincides with the foot of the Jebel Bou Naceur, where Jurassic rocks of the Middle Atlas overthrust Tertiary and Quaternary fanglomerates at the foot of Jebel Bou Naceur range (jebel is Moroccan for mountain) (Fig. 1b). The Jebel Bou Naceur is a mountain ridge with a maximum elevation of 3356 m.a.s.l., rising ~2500 m above the Moulouya basin, which is limited by a southeastern facing topographic scarp that Delcaillau et al. (2008) interpreted as an active fault zone. The Neogene–Quaternary basin fill onlaps the undeformed Jurassic bedrock of the High Plateaus on the eastern margin of the Missour basin. Plio–Pleistocene lacustrine deposits overlap much of the Jurassic carbonates of the High Plateaus. The timing of initial thrusting at Jebel Bou Naceur is unknown, but according to Laville et al. (2007), the thrust system was active during the Neogene, when Mesozoic rocks were thrust over fluvial rocks of the Bou Irhardaiene Formation. Paleomagnetic data reported by Krijgsman and Langereis (2000) suggest that the deposit of the Bou Irhardaiene Formation lasted till the lower Pliocene (Zanclean). Thrust-related folding occurs in the northwestern margin of the basin and deforms the Bou Irhardaiene Formation and Quaternary alluvial gravels; the gravels are unconformable in some places (Delcaillau et al., 2008).

The mean elevation of the Middle Atlas mountains (between 1500 and 2000 m) contrasts with its crustal thickness, recently determined in ca. 32 km by a wide-angle seismic survey (Ayarza et al., 2014). The relatively thin crust suggests a modest degree of crustal thickening, which is consistent with the amount of observed shortening, and provides support to the view that the crust is not isostatically equilibrated at crustal level. To explain this discrepancy, the subcrustal structure was investigated by means of potential-field modeling, which indicated that the lithosphere was thin (<90 km) under the Middle Atlas mountains and the Arhbalou–Missour basins (Fullea et al., 2010; Teixell et al., 2005; Zeyen et al., 2005), an inference recently confirmed by seismological data (Miller and Becker, 2014; Palomeras et al., 2014). Hence, surface uplift of the Atlas region is divided into two components: a component of crustal isostasy related to (modest) thickness variations of the crust during the Atlas orogeny, and a component related to changes in mantle buoyancy, probably due to an asthenospheric upwelling (which was described as dynamic topography by Teixell et al., 2005, and Sun et al., 2014). The first component is circumscribed to the High

and Middle Atlas deformed belts, whereas the second is of longer wavelength and affects also the peripheral Arhbalou and Missour basins. On the basis of unconformable, Messinian-age marine deposits at high altitude, Babault et al. (2008) estimated the magnitude of post-Miocene mantle-driven rock uplift in the Middle Atlas is ~1000 m. Furthermore, geomorphic indexes from the lower Moulouya river led Barcos et al. (2014) to suggest that this component of uplift is still active.

3. Methods

3.1. Knickpoints and paleoprofile reconstruction

The river profiles shown in this paper are based on the Digital Elevation Model (DEM) with 90 m of pixel resolution provided by the Shuttle Radar Topography Mission (SRMT) from the National Aeronautics and Space Administration (NASA).

The term knickpoint describes an abrupt change in river gradient, which creates a local convexity in the generally concave-up idealized graded stream longitudinal profile (Whipple and Tucker, 1999). The term knickzone is used when the convex segment of the river longitudinal profile persists along some kilometers. In our analysis, we consider the present-day position of knickpoint as due to an incision wave related to base level fall by comparing the current longitudinal profile with a reconstructed past hypothetical ideal longitudinal profile (paleoprofile). Therefore, we use paleo-longitudinal river profiles as a proxy for surface uplift. A paleo-longitudinal river profile can be determined for the segment located upstream of a knickpoint by using the equation proposed by Hoke et al. (2007). This approach implies that knickpoint separates an unmodified upstream segment from a downstream one that adapts its slope to the new boundary conditions imposed by the base level fall (Bishop, 2007; Whipple and Tucker, 1999). It is also assumed that the upstream segment (headwater from the knickpoint) was equilibrated to the conditions prior to the base-level fall. Under these assumptions, the empirical power-law gradient–area relationship (Flint, 1974; Howard and Kerby, 1983) together with the relationship between downstream distance, x , and cumulative drainage area (Hack, 1957), can be used to reconstruct a paleo-longitudinal river profile from the equation (Whipple, 2001; Whipple and Tucker, 1999):

$$z(X) = k_s k_a^{-\theta} (1 - h\theta)^{-1} (L^{1-h\theta} - x^{1-h\theta}) + z(L) \quad h \neq 1; \quad x_c \leq x \leq L; \quad (1)$$

where $z(X)$ is the elevation z at a distance X from drainage divide, L is the distance from the outlet to the drainage divide, x_c is the distance from the divide at which fluvial processes become dominant over hill-slope processes, k_s is the steepness index, θ is the concavity index, k_a is Hack's (1957) coefficient and h is Hack's (1957) exponent. The difference in elevation between the paleo profile and the present-day downstream segment at the outlet gives the knickpoint height. We have reconstructed the unmodified upstream segment profile (inherited from the old boundary conditions), which allowed us to obtain values for k_s and θ , and used these values to the downstream segment, affected by the new boundary conditions.

3.2. Surface dating

We have dated two alluvial fan/terrace surfaces (T1 and T2) in the Chegg Ard valley, which traverses the Middle Atlas and the eastern Missour basin. The surfaces dated in this study were mostly composed of pebbles, cobbles, and occasional small boulders limestone and dolostone. However, there are also minor amounts of sandstone and phyllite cobbles. We selected cobbles of sandstone and phyllite for ^{10}Be TCN dating. The sampled surfaces are flat and extensive, and unaffected by topographic shielding. Samples were collected from sites far enough from hill slopes as to minimize material gained from upper

Table 1
Sample numbers, descriptions, locations, ^{10}Be data, and ^{10}Be ages for surfaces in the Chegg Ard valley.

Sample number	Surface	Lithology	Class size Height/width/length (cm)	Sample thickness (cm)	Latitude (°N)	Longitude (°E)	Altitude ¹ (m.a.s.l)	Topographic correction	^{10}Be concentration ² (atoms/g SiO_2 $\times 10^4$)	Age Time independent Lal (1991)/Stone (2000) ^{3,4} (ka)	Age Desilets and Zreda (2003), Desilets et al. (2006) ⁵ (ka)	Age Dunai (2001) ⁵ (ka)	Age Lifton et al. (2005) ⁵ (ka)	Age Time dependent Lal (1991)/Stone (2000) ⁵ (ka)	Age Time dependent Lal (1991)/Stone (2000) ⁵ applying 1.4 m/Ma erosion (ka)
M908	T1a	Quartzite	12/8/5	5	33.36906667	-3.880783333	1144	1	383 ± 8	473.6 ± 47.8 (11.5)	464.5 ± 62.7	447.2 ± 59.8	444.4 ± 50.2	424.1 ± 41.1	n/a
M909	T1a	Sandstone	35-long	5	33.36913333	-3.88035	1140	1	351 ± 11	431.8 ± 44.4 (14.9)	421.9 ± 57.3	404.5 ± 54.4	401.5 ± 45.9	385.5 ± 38.2	n/a
M910	T1a	Sandstone	17/11/8	5	33.36906667	-3.88035	1143	1	351 ± 9	430.7 ± 43.6 (12.7)	420.5 ± 56.5	403.2 ± 53.8	400.3 ± 45.2	384.5 ± 37.5	n/a
M911	T1a	Sandstone	15/8/5	5	33.36893333	-3.879966667	1145	1	464 ± 13	590.6 ± 62.6 (18.9)	573.3 ± 80.4	553.1 ± 76.8	549.8 ± 46.7	528.5 ± 53.6	n/a
M912	T1a	Sandstone	10/8/05	5	33.36965	-3.879683333	1147	1	355 ± 11	435.0 ± 44.8 (15.0)	425.2 ± 57.7	407.3 ± 54.8	404.4 ± 46.3	388.1 ± 38.4	n/a
M913	T1a	Sandstone	15/10/5	5	33.36973333	-3.87945	1147	1	364 ± 12	446.4 ± 46.3 (16.0)	437.4 ± 59.7	419.6 ± 56.8	416.2 ± 48.0	397.8 ± 39.7	n/a
M915	T1b	Sandstone	14/10/5	5	33.37775	-3.896533333	1208	1	392 ± 11	463.0 ± 47.5 (14.5)	451.4 ± 61.4	434.5 ± 58.5	431.1 ± 49.3	412.3 ± 40.6	n/a
M916	T1b	Sandstone	17/10/6	6	33.37796667	-3.897616667	1212	1	363 ± 9	427.0 ± 43.1 (12.3)	413.4 ± 55.4	397.4 ± 52.8	394.4 ± 44.4	380.3 ± 36.9	n/a
M917	T1b	Sandstone	11/7/05	5	33.37855	-3.897766667	1211	0.8542	345 ± 8	474.4 ± 48.3 (12.9)	462.7 ± 62.7	445.9 ± 59.9	442.6 ± 50.3	424.1 ± 41.4	n/a
M918	T1b	Sandstone	15/11/5	5	33.37838333	-3.89695	1209	1	316 ± 10	363.5 ± 36.8 (12.4)	348.1 ± 46.4	335.4 ± 44.3	332.5 ± 37.4	320.9 ± 31.3	n/a

M919	T1b	Sandstone	11/9/04	4	33.37893333	-3.898333333	1214	1	451 ± 15	534.1 ± 56.9 (20.4)	521.0 ± 72.9	501.3 ± 69.5	498.1 ± 58.8	478.6 ± 49.0	n/a
M920	T2a	Sandstone	17/13/6	6	33.39696667	-3.905066667	1134	1	45 ± 2	50.8 ± 5.3 (2.7)	49.8 ± 6.5	48.6 ± 6.3	47.8 ± 5.4	45.7 ± 4.6	48.5 ± 5.1
M921	T2a	Sandstone	13/7/4	4	33.39696667	-3.905083333	1135	1	73 ± 2	81.5 ± 7.5 (1.9)	80.9 ± 9.9	78.6 ± 9.6	77.8 ± 8.0	74.3 ± 6.6	81.7 ± 8.1
M922	T2a	Sandstone	13/8/6	6	33.39696667	-3.905	1135	1	51 ± 3	57.3 ± 5.8 (2.9)	57.1 ± 7.4	55.6 ± 7.2	54.7 ± 6.1	51.9 ± 5.2	55.8 ± 5.9
M923	T2a	Sandstone	15/12/7	7	33.39673333	-3.905066667	1134	1	59 ± 3	67.5 ± 6.8 (3.2)	67.0 ± 8.7	65.4 ± 8.4	64.7 ± 7.2	61.8 ± 6.1	66.6 ± 7.1
M924	T2a	Sandstone	9/7/06	7	33.3967	-3.9048	1135	1	69 ± 5	79.3 ± 9.5 (6.4)	78.6 ± 11.4	76.4 ± 11.0	75.6 ± 9.7	72.3 ± 8.5	79.2 ± 10.3
M925	T2a	Sandstone	12/8/05	5	33.39643333	-3.90445	1134	1	42 ± 10	47.0 ± 12.0 (11.2)	46.0 ± 12.3	45.1 ± 12.0	44.4 ± 11.5	42.6 ± 10.8	44.8 ± 12.0
M926	T2b	Siltstone	26/18/7	7	33.35616667	-3.856266667	1018	0.8542	236 ± 10	368.5 ± 39.3 (17.5)	360.2 ± 49.6	345.8 ± 47.2	343.6 ± 40.4	327.8 ± 33.8	671.5 ± 193.2
M927	T2b	Phyllite	7/7/07	7	33.35606667	-3.856516667	1021	1	92 ± 3	116.4 ± 11.3 (4.5)	113.7 ± 14.5	110.7 ± 14.0	109.7 ± 11.9	105.1 ± 10.0	119.7 ± 13.2
M928	T2b	Sandstone	20/7/7	7	33.35596667	-3.857266667	1022	1	48 ± 2	59.8 ± 5.8 (2.5)	60.2 ± 7.6	58.7 ± 7.4	57.9 ± 6.3	54.6 ± 5.2	58.8 ± 6.0
M929	T2b	Sandstone	20/10/4	4	33.35536667	-3.855733333	1016	1	17 ± 1	21.1 ± 2.1 (1.0)	22.7 ± 2.8	22.4 ± 2.9	22.1 ± 2.4	20.4 ± 2.0	20.9 ± 2.1
M930	T2b	Sandstone	18/8/5	5	33.35615	-3.857966667	1021	1	69 ± 3	84.5 ± 8.2 (3.3)	84.6 ± 10.7	82.2 ± 10.4	81.4 ± 8.8	77.3 ± 7.3	85.3 ± 9.0
M932	T2b	Sandstone	16/8/6	6	33.35588333	-3.853433333	1012	1	19 ± 2	22.7 ± 2.7 (1.9)	24.3 ± 3.5	24.0 ± 3.5	23.7 ± 3.1	22.0 ± 2.6	22.5 ± 2.7
													Average ⁶	52 ± 20	

¹ Altitudes were determined using a handheld GPS with an uncertainty of ± 30 m.

² Six blanks were measured with $^{10}\text{Be}/^9\text{Be}$ ratio = $4.24 \pm 2.3 \times 10^{-14}$.

³ Ages were determined using a rock density of 2.75 g/cm³ and 07KNSTD standard. Uncertainties include analytical and production rate/scale model uncertainties.

⁴ Uncertainty includes analytical and production rates and uncertainty in parenthesis is only analytical.

⁵ Samples M926 and M927 were not included in average.

levels. We also selected sampling sites with little evidence of erosion, generally in areas with well-developed rock varnish. The sampled cobble was 5–10 cm-tall and 10–20 cm in diameter (Table 1).

Samples were prepared at the TCN Geochronology Laboratories of the University of Cincinnati. About 500 g of each sample was crushed and sieved to obtain 250–500 μm fraction, from which quartz was separated using the methods of Kohl and Nishiizumi (1992). Be carrier was added to each sample, and by means of an ion exchange chromatography technique, Be was separated, purified and precipitated as $\text{Be}(\text{OH})_2$ at a pH 7. The $\text{Be}(\text{OH})_2$ gel was calcinated by ignition at 750 °C for 5 min in quartz crucibles. The resultant BeO was mixed with Nb powder and loaded into steel targets. $^{10}\text{Be}/^{9}\text{Be}$ ratios were measured with accelerator mass spectrometry at the Purdue Rare Isotope Measurement Laboratory of the Purdue University. Isotope ratios were compared with ICN Pharmaceutical Incorporated ^{10}Be and NIST (National Institute Standard of Technology) standards prepared by K. Nishiizumi.

Ages were calculated with CRONUS-Earth online calculator Version 2.2, applying appropriate ^{10}Be standardizations (Balco et al., 2008) with a sea-level high latitude (SLHL) production rate of 4.49 ± 0.39 ^{10}Be atoms g^{-1} of quartz yr^{-1} , a ^{10}Be half-life of 1.36×10^6 years (Nishiizumi et al., 2007) and a rock density of 2.75 g cm^{-3} at zero-erosion rate.

There is currently much debate regarding the appropriate scaling models and geomagnetic corrections to calculate surface exposure ages from TCN production (e.g., Pigati and Lifton 2004; Staiger et al. 2007; Balco et al., 2008). We present ages for all scaling models, but choose those of Lal (1991) and Stone (2000) in our discussion (Table 1). However, we are aware that other scaling models would produce ages that may be up to 10% older (Table 1).

3.3. Quantifying fluvial incision and deformation rates

Incised fluvial surfaces allow fluvial incision rates (I) to be estimated by using the age (A) and height (h) of the surface with respect to the present-day position of the river channel, such that $I = h/A$ (e.g., Burbank and Anderson, 2001). In this work, the absolute elevation of terrace surfaces (h) as obtained from the SRTM90 DEM, whose precision is optimal when measuring surfaces with slopes $< 10\%$ (Gorokhovich et al., 2006). The accuracy decreases when measuring the absolute elevation of surfaces narrower than 180 m, as occurs in some parts of the river channel and locally in terraces. In these cases, the elevation data have been contrasted with field measurements obtained with a conventional altimeter. Although absolute elevation values requires frequent calibration (according to atmospheric conditions), in our analysis we do not use absolute elevation data, but elevation difference between terrace surfaces and present-day river channel. Thus, altimeter accuracy is approximately 1 m when the elevation of two surfaces is measured in a short time lapse. Relative structural uplift has been calculated by comparing the relative elevation of a geomorphic surface with respect to the present-day river channel at both sides of a tectonic flexure, thus assuming that the original surface sloped at a gradient similar to today's stream.

4. River profiles and knickpoint analysis

4.1. Moulouya river

The Moulouya river profile is not the typical concave up shaped denoting equilibrium, but it shows a series of knickpoints. The upper reach of the Moulouya river flows over its own alluvial deposits through a wide valley, presenting a surprisingly gentle gradient of 0.16° along 50 km, after which slope abruptly increases (gradient $> 0.3^\circ$) for about 10 km defining a 80 m-high knickpoint (Fig. 2b). The knickpoint coincides with scarcely erodible Paleozoic granitic bedrock. Downstream, the Moulouya river flows again over alluvial deposits and shows its gentle slope until its confluence with the Asseghmir river. The Asseghmir

river drains $\sim 1350 \text{ km}^2$ of the northern flank of the High Atlas, representing a third of the total drainage area of the Moulouya river downstream of their confluence. The Asseghmir river has a knickpoint of similar characteristics to those on the Moulouya river (Fig. 2a), though located in the northern flank of the High Atlas Mountains at an elevation $\sim 300 \text{ m}$ higher than in the Moulouya river. From the tributary junction, the Moulouya river flows east for almost 50 km across Jurassic limestone, granite and slate of the Aouli Massif, showing a steeper gradient of 0.38° until it reaches the Tamdafelt fold system (Figs. 1 and 2a). This steeper segment defines a knickzone that is 300–400 m-high (Fig. 2b). The Enjil river joins the Moulouya downstream this knickzone, also depicting a knickzone, located close to the confluence (Fig. 2a).

Downstream from the Tamdafelt fold system (Fig. 1), the Moulouya river flows along the Missouri sedimentary basin where its gradient becomes gentle again, averaging 0.14° for $> 150 \text{ km}$. A slight increase in gradient occurs again at the boundary between the Missouri and Guercif basins, where the river cuts Jurassic dolostones, but the gradient becomes gentler in the Guercif basin, averaging 0.12° until the outlet. Along the Missouri and Guercif basins, the Moulouya river joins tributaries, that drain both the High Plateaus and the Middle Atlas (Jebel Bou Naceur), the most important one being the Za river.

4.2. Streams draining the High Plateaus

The western edge of the High Plateaus is drained by tributaries of the Moulouya, which have significant knickzones (red reaches in Fig. 3). Fig. 4a shows the profiles of the Moulouya river and its tributaries, all shearing the same distance to the Mediterranean outlet. All profiles have gentler slopes in their upper courses (generally $< 0.2^\circ$), with an abrupt slope increase along their middle courses, and progressively gentler slopes downstream. The gentle gradient of the upper segments suggests that little channel incision has occurred upstream of the knickpoints, and therefore these upper course gradients can be interpreted as inherited from the Missouri basin paleosurface. In this case, the lateral correlation of these gentle gradients allows us to delineate a paleosurface reaching 500–550 m above the present Moulouya river (Fig. 4a). The knickpoints for the Fajane and Kaddou tributaries, draining the High Plateaus into the Missouri basin, are 500 and 550 m-high, respectively (Fig. 4b and c). The Za river is the main tributary of the Moulouya river, draining $\sim 20,000 \text{ km}^2$ of the High Plateaus to the lower Guercif basin. The upper Za course is $\sim 300 \text{ km}$ -long into the Plio–Pleistocene fluvial deposits of the High Plateaus, with entrenchments of $\sim 100 \text{ m}$ close to the knickzone. The gradient of the upper course is 0.15° , while downstream, the gradient increases to 0.33° for almost 80 km at the eastern edge of the Guercif basin that is composed of Jurassic carbonates and shows a 400–450 m-high knickzone (Fig. 4d). Considering an average entrenchment of 100 m for the Za river into the Guercif basin, the total height of this knickpoint is 500–550 m.

4.3. Streams draining the Jebel Bou Naceur

The Chegg Ard, El Mansoor, El Berd and Timrhout rivers drain the southeastern Jebel Bou Naceur into the Missouri and Guercif basins (Fig. 3). The Chegg Ard has a catchment area of $\sim 240 \text{ km}^2$ upstream the Missouri basin, showing an impressive 1000 m-high knickpoint (Fig. 5a), located at approximately the contact between Toarcian marls and overlying Bathonian–Callovian sandstone (Charroud, 2002). The upper course of the Chegg Ard river flows for $\sim 10 \text{ km}$ on a wide valley (Fig. 5b), where the channel is slightly entrenched and has a gradient of 1.3° . Downstream, channel gradient abruptly increases to 3.1° and is deeply entrenched. Finally, the Chegg Ard river has an average gradient of 0.9° from the knickpoint to the confluence with the Moulouya river.

Tributary streams that flow parallel to the structural grain of the Middle Atlas drain the eastern edge of the Jebel Bou Naceur. These tributaries converge downstream to become the Melloulou river, which, in

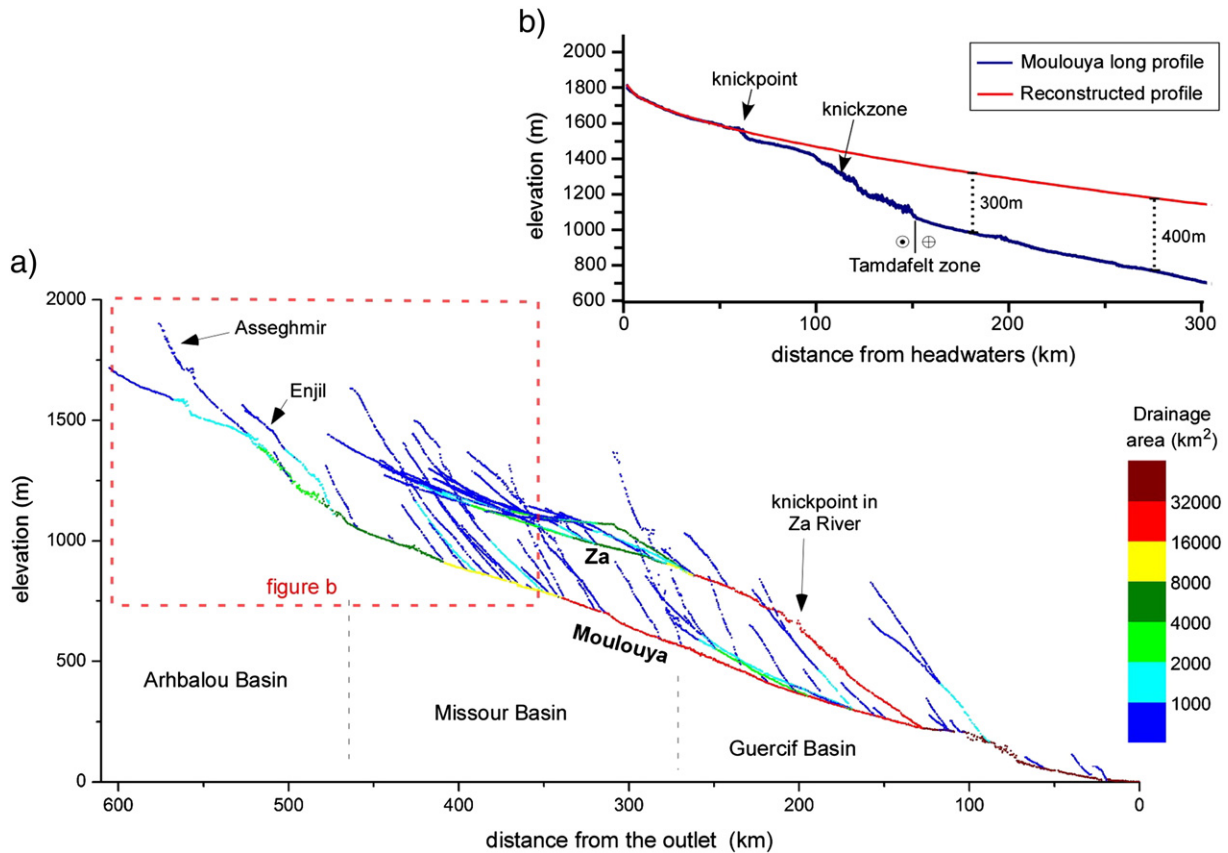


Fig. 2. a) Profiles of the Moulouya river system from headwaters to the Mediterranean. The color bar indicates the area of the upstream drainage area. b) Profile of the Moulouya river in the Arhbalou and Missouri basins, showing a knickzone located 100–150 km from the headwaters. The reconstructed profile (using $K_s = 21$ and $\theta = 0.24$) shows a difference in elevation of 300–400 m with respect to the current river channel.

turn, joins the Moulouya river in the central Guercif basin. Tributaries of the Melloulou river include the El Mansoor, El Berd and Timrhout rivers, which have large knickpoints in their mountainous courses with heights of 700–800 m (Fig. 5c and d). The channel of the Timrhout river has been blocked by a rock-slide to form a lake (Gualta Tamda; Fig. 5e). The location of the rock-slide coincides with the upper segment of an 800 m-high knickpoint, thus suggesting that slope instability may have been partially triggered by rapid fluvial incision.

5. Quaternary fluvial surfaces in the lower Chegg Ard valley

Alluvial fan surfaces and fluvial terraces along the Chegg Ard, the main river draining the Jebel Bou Naceur to the Missouri basin, were selected for dating because they preserve a good record of fluvial deposits and exhibit signs of recent deformation related to folds associated with the southern Middle Atlas thrust front (Fig. 6) (Delcaillau et al., 2008; Laville et al., 2007). Four sets of fluvial deposits and abandoned alluvial fan surfaces were mapped along the Chegg Ard valley, which we have named T1 (oldest) to T4 (youngest) (Figs. 6 and 7).

The T1 is an extensive alluvial fan surface, which has a radial length of ~12 km with its apex located near the mountain front, at the boundary between the Middle Atlas Mesozoic carbonate rocks and the Tertiary clastic deposits of the Missouri basin. This alluvial fan surface is entrenched by the Chegg Ard channel to a depth of 135–185 m. The surface is defined by 1–5 m thick fanglomerate level, which conformably overlies Tertiary conglomerates of the Bou Irhardaiene Formation. The T1 fanglomerate is composed of cobbles and boulders that become smaller downstream. Locally, in the upper areas of the abandoned alluvial fan, old longitudinal bars composed of >50 cm-diameter imbricated boulders are observed, suggesting of a highly energetic depositional environment. The clasts mainly comprise carbonate rocks. The T1 surface

also shows well-developed pedogenic carbonate cement (Stage V of Gile et al., 1981). The alluvial fan is almost completely eroded southward of the frontal monocline fold (FMF; Fig. 6), being restricted to small patches in the forelimb. Stratified conglomerates abutting the forelimb of the FMF, which are unconformable on the Bou Irhardaiene Formation conglomerates, may be the sole distal remnants of T1 at the foot of the FMF. The presence of embedded deposits suggests a relative base level drop, and we assume that remnants of T1 had to be formed above the T2, at least 35 m above the present-day channel height.

The abandoned fluvial and alluvial surface T2 is present in three locations along the Chegg Ard valley (Fig. 6b). The main exposure occurs south of the FMF, where it forms a large lobe of an alluvial fan that extends for 14 km until it reaches the Moulouya river (T2b). Other remnants are present as river terraces in the cores of the FMF and the Beni Aioun anticline (T2c and T2a; Figs. 6a and 7a). The T2 deposits have the same general characteristics as T1, but the average size of the clasts is smaller, rarely reaching >20 cm in diameter. T2 usually shows moderate pedogenic carbonate development (carbonate morphology stages III–IV of Gile et al., 1981). The T3 and T4 deposits are well preserved south of the FMF, displaying similar features to T2, though carbonate cement is less developed. T3 is composed of decimeter-size clasts, some of them reaching 30 cm in diameter, whereas T4 has smaller clasts (rarely reaching 15 cm in diameter).

6. ^{10}Be terrestrial cosmogenic nuclide results

6.1. Erosion rate estimates

TCN concentrations can be used to estimate steady-state erosion rates (erosional equilibrium; Lal, 1991). Thus, samples with higher TCN concentrations provide lower limits on erosion rates. We have

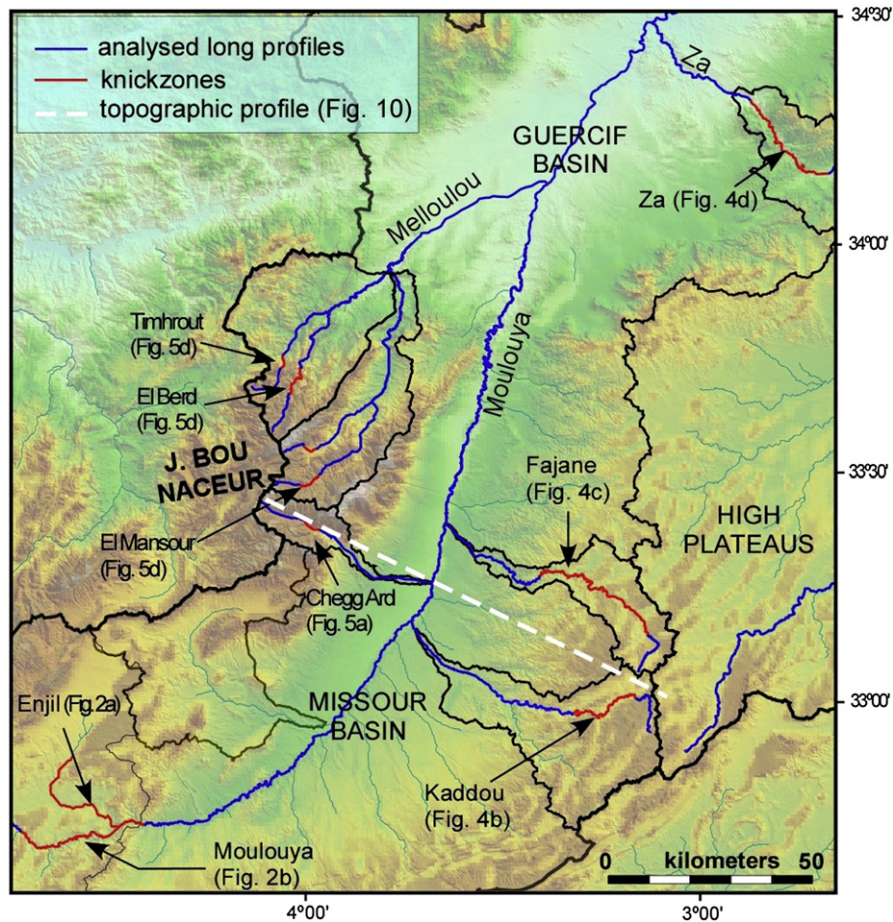


Fig. 3. Digital elevation model (DEM SRTM90) for the Missouri and Guercif basins (central segment of the Moulouya river). The river courses analyzed in this study are highlighted. The dashed white line marks the location of the topographic profile shown in Fig. 10.

used ^{10}Be concentrations in the clasts for T1 samples (except M918, which yielded an age significantly younger than the other ones) to estimate erosion rates by using the method of Lal (1991). This provides a minimum erosion-rate estimate because we preferentially selected clasts that appeared more resistant to erosion, most of them still preserving rounded fluvial shapes and an absence of notable weathering features, such as exfoliated surfaces, pitting, or granular disintegration. Moreover, T1 surface is strongly cemented, thus increasing its resistance to erosion. The ten oldest ages of surface clasts provide a mean erosion rate of $1.4 \pm 0.2 \text{ m Ma}^{-1}$, which is in good agreement with those obtained in climatically similar settings (e.g., Matmon et al., 2009; Portenga and Bierman, 2011), as discussed by Arboleya et al. (2008) in their study on terrace dating in the Ouarzazate basin.

6.2. Terrace ages in the Chegg Ard Valley

Sampled boulders may retain a signal of prior exposure with inherited TCNs, which result in ages that are older than the surface being dated (Anderson et al., 1996; Hancock et al., 1999). Intense weathering or exhumation of clasts may result in lower concentrations of TCNs, which, in turn, would underestimate the age of the surface. Collecting multiple samples from each terrace and looking for potential outliers, that is, exposure ages that fall significantly outside the mean value ($>2 \sigma$) of all the ages obtained for a given landform, can help to identify the problem of derived and/or weathered/exhumed boulders. We have used the erosion rates estimates based on the oldest ten ages of surface clasts (as described in the previous sub-section) as a test to

assess the likely effects of erosion on the samples used to define the surface ages. For samples having an erosion rate of 1.4 m Ma^{-1} , a calculated age of 10 ka would underestimate the true age by a ~1%, an age of 50 ka by ~5%, an age of 100 ka by ~10%, and an age of 300 ka by ~50%. Given the uncertainties in defining the erosion rate, we have plot all our ages with zero erosion, but also present them in Table 1 for an erosion rate of 1.4 m Ma^{-1} , which places an upper limit on the possible ages.

Terrace T1 has been dated by using 11 samples from two different localities (T1a and T1b in Fig. 6), which yield ages from 321 to 528 ka (Fig. 8), with a mean age of $411 \pm 55 \text{ ka}$ (uncertainty = 1σ). The sampled clasts of sandstone and phyllite were carefully selected from the surface, mainly composed of carbonate rocks. Since the sampled clasts were well rounded, retaining their original shape, we argue that they have not undergone significant weathering. Twelve samples were dated on T2 terrace at two different localities (T2a and T2b in Figs. 6 and 7a), yielding ages between 20 and 327 ka (Fig. 8). Samples M926 ($327.8 \pm 33.8 \text{ ka}$) and M927 ($105.1 \pm 10.0 \text{ ka}$) are considered outliers since they are $>2 \sigma$ older than the mean age of the rest of the population. The presence of conglomerate clasts at locality T2b reworked from T1 or from the Bou Irhardaiene Formation supports the view that M926 and M927 have been derived from an older surface. Omitting the ages of M926 and M927, the T2 terrace has a mean age $52 \pm 20 \text{ ka}$ (uncertainty = 1σ). Two other samples, M929 and M932, fall outside the mean value ($>2 \sigma$) with ages of $20.4 \pm 10.0 \text{ ka}$ and $22.0 \pm 2.6 \text{ ka}$. We recognize that these younger age samples might have been exhumed, although we cannot prove this assumption. Omitting the ages of M929 and M932 too, the T2 terrace has a mean age $62.6 \pm 14.1 \text{ ka}$

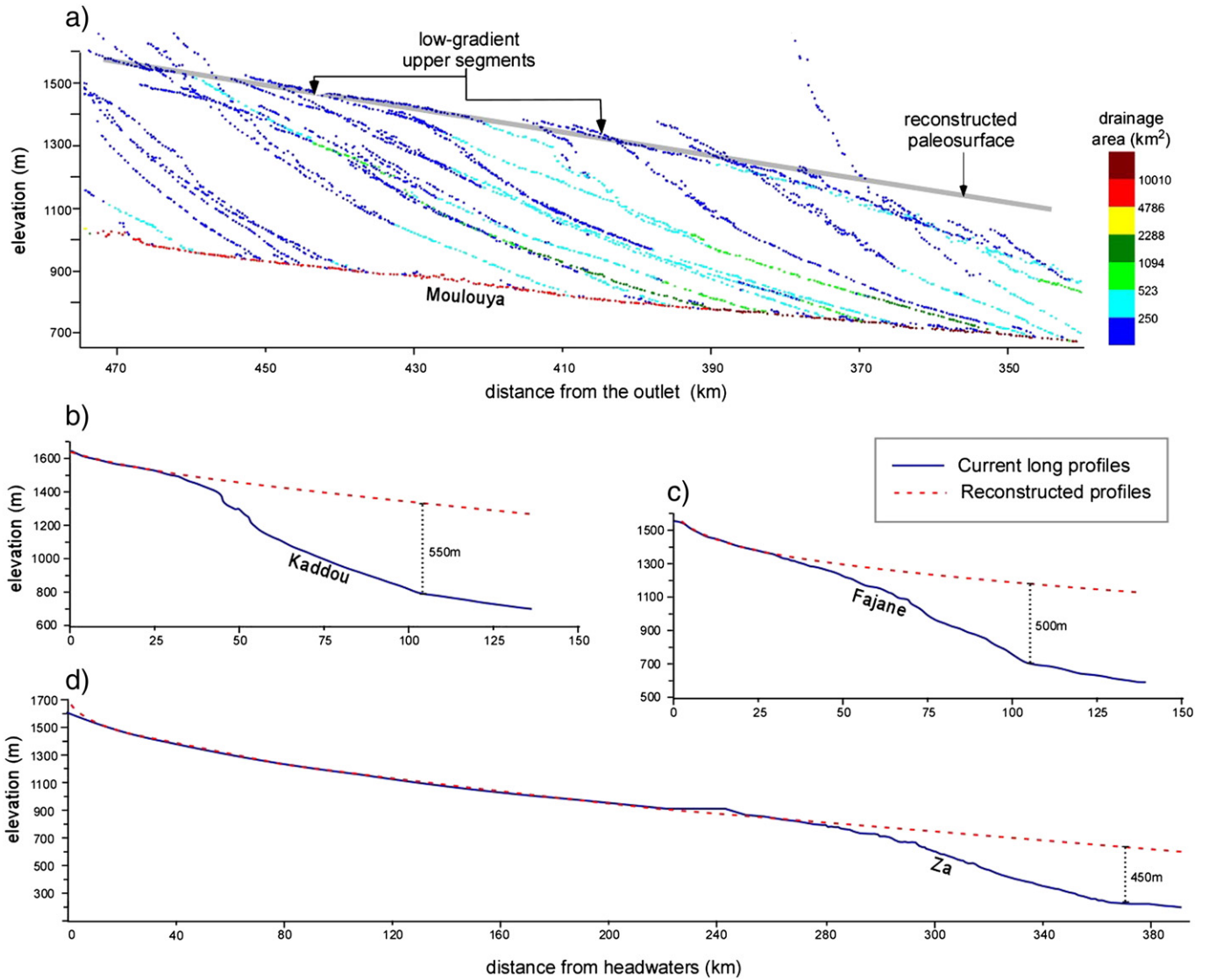


Fig. 4. (a) Profiles for the Moulouya river and its tributaries with drainage areas over 50 km² projected on the same plane. Most of the tributaries draining the stable margin of the Missouri basin exhibit anomalously low gradients in their upper courses and similar knickzones. The prolongation of these upper courses allows reconstructing the basin paleosurface, which was 500–550 m above the current Moulouya river channel. (b) Profile of the Kaddou river (see location in Fig. 3) draining the stable margin of the Missouri basin; red dashed line shows the reconstructed paleoprofile (using $K_s = 13$ and $\theta = 0.19$) that reaches 550 m over the current Moulouya river. (c) Profile of the Fajane river (see location in Fig. 3); red dashed line shows the reconstructed paleoprofile with $K_s = 83$ and $\theta = 0.40$; this paleoprofile reaches 500 m over the Moulouya river channel. (d) Profile of the Za river (see location in Fig. 3) draining the High Plateaus to the Guercif basin; red dashed line shows the reconstructed paleoprofile using $K_s = 34$ and $\theta = 0.26$, which reaches 450 m over the Moulouya river channel.

(uncertainty = 1 σ). In the following we will use the older mean value for the age of T2 (62 ± 14 ka).

6.3. Tectonic uplift and incision rates

The dated T1 and T2 terraces are incised by the Chegg Ard river in different places along the Chegg Ard Valley, where incision can be measured in both the tectonically uplifted area of the basin margin and the central Missouri basin. The FMF and Beni Aioun anticline (Fig. 6) have deformed the upper segments of terraces T1 and T2. The FMF is the frontal-most structure of the Middle Atlas, being located ~12 km downstream from the mountain front. This SE-vergent fold trends SW–NE and shows an almost horizontal backlimb and a subvertical forelimb, whereas the Beni Aioun anticline (BAA in Fig. 6) is a gentle anticline located between the mountain front and the FMF.

Immediately northwards of the FMF in the tectonically uplifted fold limb, T1 surface is 133 ± 3 m above the current river channel (Fig. 9). T1 is also tilted by the Beni Aioun anticline and reaches 182 ± 5 m above the current river channel near the mountain front (Fig. 9). Thus, incision rates measured from T1 in the tectonically uplifted area range from 0.32 ± 0.04 to 0.44 ± 0.06 mm yr⁻¹ (Fig. 9). The difference between these rates is ~0.1 mm yr⁻¹, and is likely due to the local uplift generated by the Beni Aioun anticline.

Surface T2 is not continuously preserved along the Chegg Ard valley and shows very little deformation, though its elevation with respect to the current river channel significantly varies along the valley. Thus, T2 is present in the cores of FMF and Beni Aioun anticline, being at ~51 to 55 m above the present-day channel respectively (T2c and T2a in Figs. 6b and 7a; Fig. 9). T2 also forms the alluvial fan located downstream from the FMF, being incised ~16 \pm 3 m in the distal course and 32 \pm 3 m in its upper one (T2b in Figs. 6b and 7a; Fig. 9). The

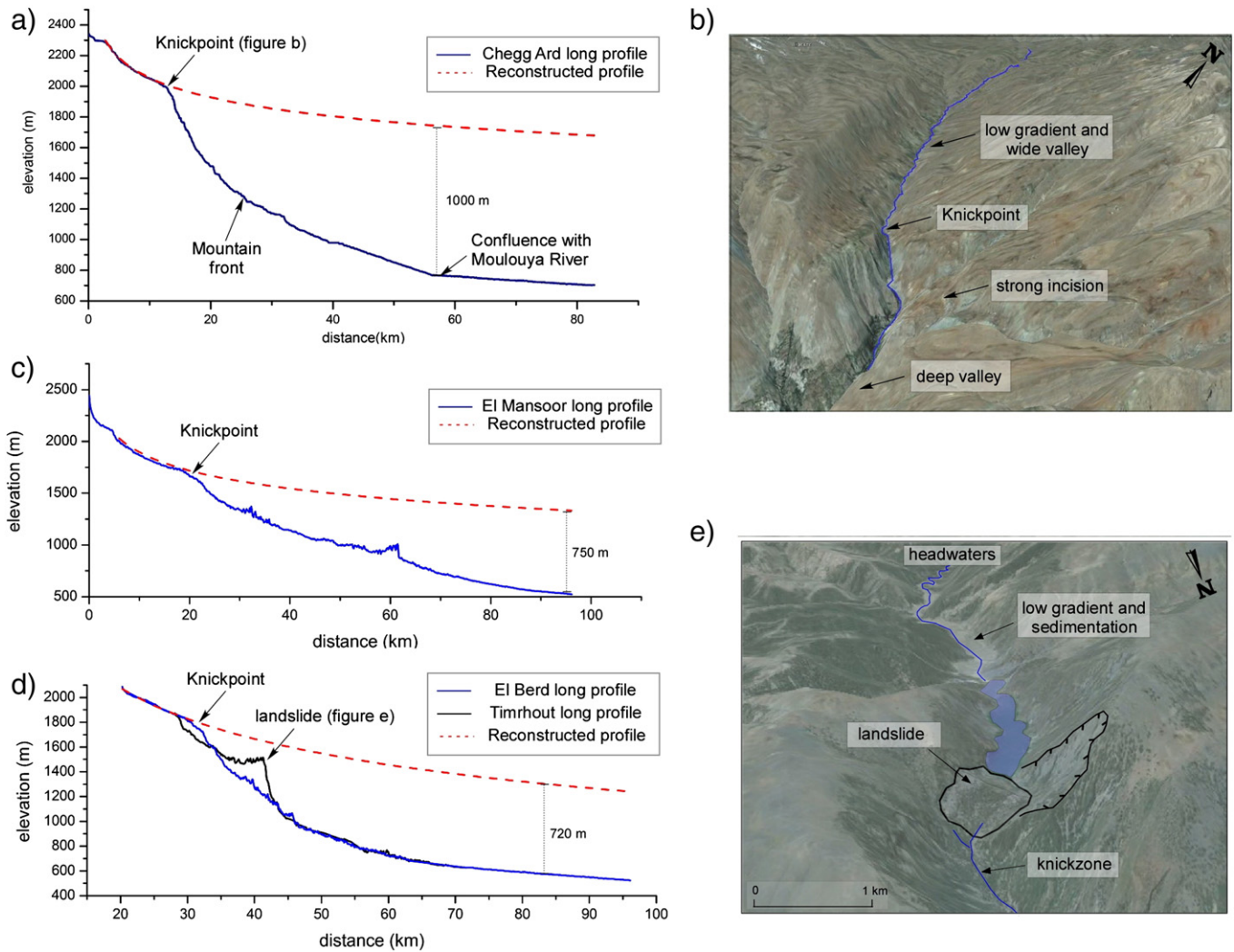


Fig. 5. (a) Profile of the Chegg Ard river (see location in Fig. 3), which drains the Jebel Bou Naceur to the Missouri basin. Red dashed line shows a reconstructed paleoprofile (using $K_s = 680$ and $\theta = 0.62$) that reaches 1000 m over the current Moulouya river channel. (b) Satellite image from Google Earth of the mountainous course of the Chegg Ard river. Upstream the channel flows along a wide valley; downwards the profile exhibits a large knickpoint, downstream from which the channel is deeply incised. (c) Profile of the El Mansoor river (see location in Fig. 3), which drain the Jebel Bou Naceur to the Guercif basin. Red dashed line shows a reconstructed paleoprofile (using $K_s = 950$ and $\theta = 0.62$) that reaches 750 m over the current Moulouya river channel. (d) Profile of the El Berd and Timrhout rivers (see location in Fig. 3), which drain the Jebel Bou Naceur to the Guercif basin. Red dashed line shows a reconstructed paleoprofile (using $K_s = 5722$ and $\theta = 0.75$) that reaches 7200 m over the current Moulouya river channel. (e) Satellite image from Google Earth showing the mountainous course of the Timrhout river blocked by a rock-slide, that created an abrupt knickpoint and the lake Gualta Tamda.

difference between these incision values, with higher incision in the apex and lower incision in distal parts of the fan, is probably mostly due to the difference in gradient between the steeper slope of the incised alluvial fan and the gentler slope of the contemporary river. Considering an age of 62 ± 14 ka for T2, we calculate incision rates that range from 0.28 ± 0.12 mm yr⁻¹ in the distal alluvial fan surface to 0.55 ± 0.17 mm yr⁻¹ in the fan apex (Fig. 9). T2c, in the core of the FMF is uplifted ~19 m with respect to the proximal parts of T2b, located 500 m downstream (Fig. 9). This difference in elevation corresponds to tectonic uplift related to the FMF since the abandonment of T2, which yields an average rate of ~0.3–0.4 mm yr⁻¹. Such a rate is comparable to those recorded for the past 250 ka in the deformed terraces of the proximal Ouarzazate basin in the foreland of the High Atlas (Pastor et al., 2012).

The incision rate calculated for terrace T1 at the backlimb of the FMF is 0.32 ± 0.04 mm yr⁻¹, which is significantly lower than that obtained from T2c and T2a (0.93 ± 0.26 mm yr⁻¹ and 0.88 ± 0.25 mm yr⁻¹ respectively; Fig. 9). We suggest that the more recent rates

(calculated from T2) are probably overestimated because of the terrace formation cycle of incision/aggradation has not been completed (aggradation of the newest riverbed terrace), as Arboleya et al. (2008) documented in the Ouarzazate basin. Therefore, the longer-term incision rates are likely more representative of tectonic uplift than recentmost ones, the latter being significantly higher due to climatic factors.

7. Discussion

7.1. Knickpoints, surface uplift and erosion in the Moulouya catchment

The analysis of river profiles reveals the systematic presence of large knickpoints or knickzones in the Moulouya river and its main tributaries. The formation and upstream retreat of knickpoints is typically understood as the dominant mode of channel adjustment in response to either regional or local perturbations due to one or more of the following triggering factors: regional surface uplift (e.g., Burbank and Anderson, 2001; Lavé and Avouac, 2001; Quezada et al., 2010; Wobus

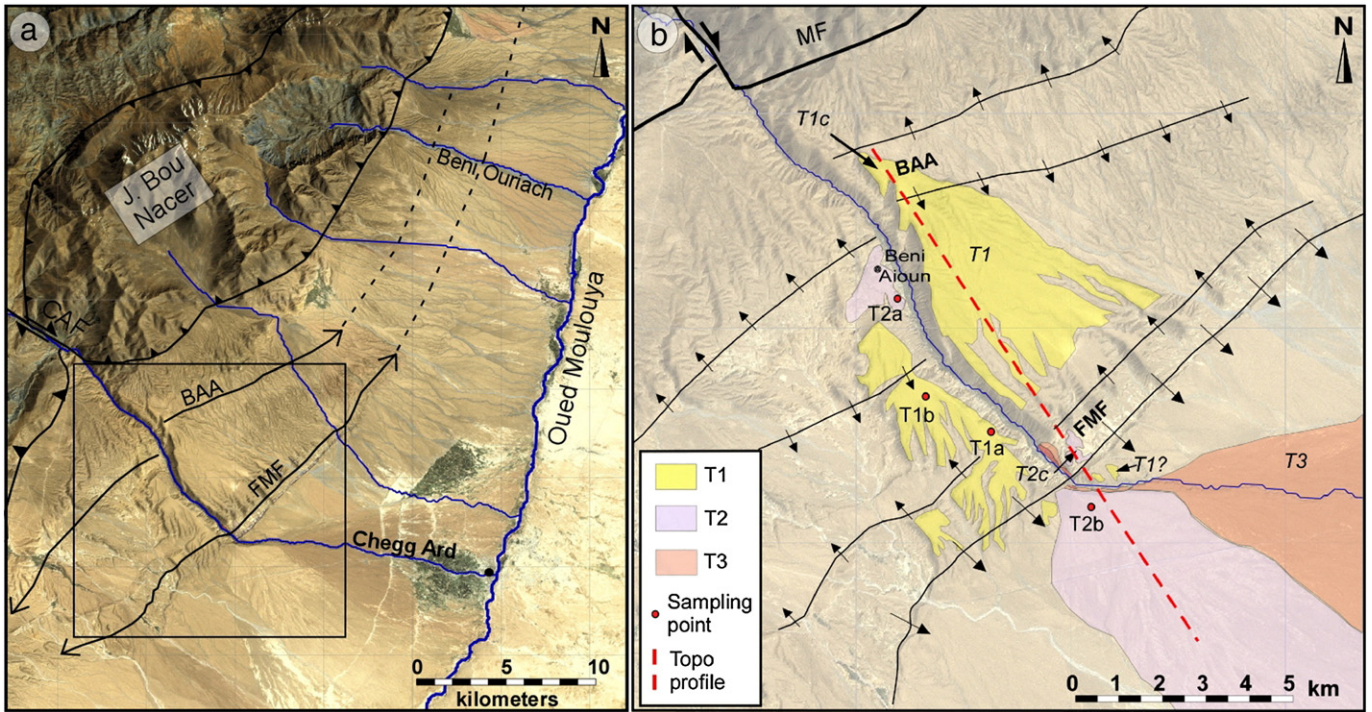


Fig. 6. (a) Google Earth image of the central Missour basin and the Jebel Bou Nacer with the main geologic structures and rivers. (b) Close-up of the Chegg Ard valley showing the mapping of fluvial deposits and landforms, tectonic flexures, sample location, and the trace of the profile in Fig. 9 (red dashed line). CAF – Chegg Arg fault; MF – mountain front; BAA – Beni Aioun anticline; FFMF – Frontal monocline.

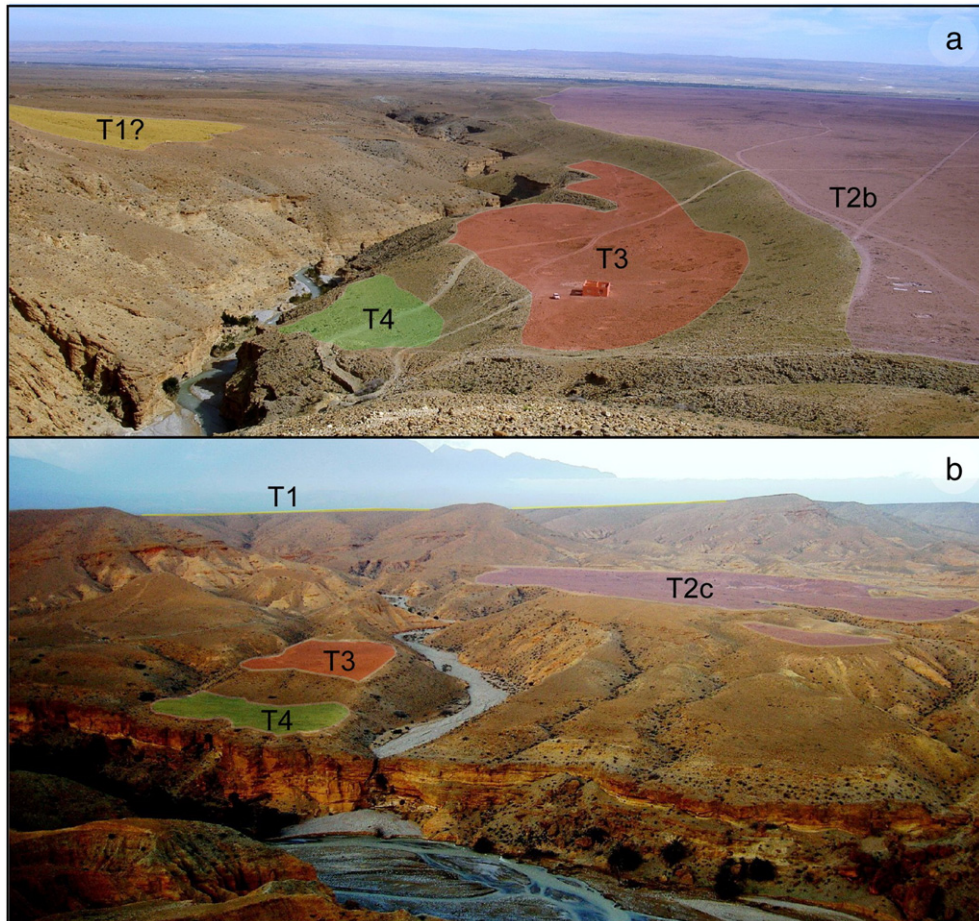


Fig. 7. Views of terrace levels at the western side of the Chegg Ard from the fold crest of the Frontal monocline. (a) View to the SE where alluvial fan surfaces T2 and T3 dominate. (b) View to the NE showing terrace T1 in the background and T2, T3 and T4 preserved in the core of the Frontal monocline.

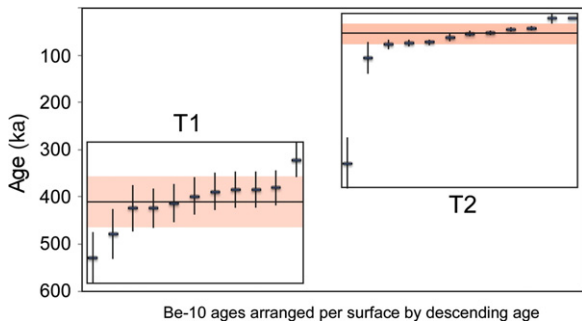


Fig. 8. Be-10 TCN ages for terrace levels T1 and T2. The horizontal black line and gray band are the mean and 1σ values for each surface.

et al., 2006), localized structural surface uplift (e.g., Burbank et al., 1996), regional base level drop (e.g., Begin et al., 1981; Snyder et al., 2002; Bishop et al., 2005; Crosby and Whipple, 2006), local base level fall directly caused by stream piracy (e.g., García, 2006) and differential erosion caused by lithological contrast (e.g., Goldrick and Bishop, 2007). Other causes may be associated with inherited relief features due to glacial erosion and/or landsliding (e.g., Benda and Dunne, 1997; Korup, 2006; Lancaster and Grant, 2006). Knickpoints in the upper Moulouya catchment near the Middle Atlas front were interpreted by Laville et al. (2007) and Delcaillau et al., (2008) as related to recent thrust deformation, without discussing the potential role of regional uplift and base level drop. Similarly, Boulton et al. (2014) has interpreted existing knickpoints in the southern High Atlas mountain front, as entirely related to active faults.

The knickpoints in the Missouri and Guercif basins are situated on tributaries draining both sides of the Moulouya river, from the stable High Plateaus to the active Middle Atlas, and must therefore be explained by a regional-scale process. This regional-scale process is most likely the adaptation of the fluvial network to the mantle-driven, long-wavelength uplift. This uplift remains active in the region (Barbero et al., 2011; Barcos et al., 2014) and has produced a maximum surface uplift of ~ 1000 m at a rate ranging from 0.17 to 0.22 mm yr^{-1} since at least the earliest Pliocene (Babault et al., 2008). The Missouri basin was still accumulating sediments (Bou Irhardaiene Formation) at early Pliocene time, after the mantle-related uplift has started. The change from internal to external drainage in the basin probably occurred when its surface was raised at a significant elevation and had accumulated potential energy enough as to be captured by a former Moulouya river with its base level located in the Mediterranean. The capture of

an endorheic basin likely triggers faster erosion rates during the first stages, which, in turn, may have caused the development of a knickpoint that propagated upwards along the entire fluvial network, until its present position at the contact between the Neogene basin fill and the Jurassic carbonate bedrock of the basin margins.

The analysis of river profiles shows that the height of knickpoints differs in the High Plateaus margin with respect to the Middle Atlas thrust front, where knickpoints present larger vertical drop. Knickpoints in rivers draining the eastern margin of the Missouri basin (adjacent to the High Plateaus), where there are no active tectonic structures, are 500 – 550 m-high at the junction with the Moulouya river (Fig. 4). This is consistent with the presence of lacustrine deposits preserved in the eastern margin of the Missouri basin at ~ 550 m above the present-day Moulouya river channel (labeled Q6 in the 1/100,000 geological map of Hassi el Ahmar and attributed to the Villafranchian -indetermined upper Pliocene; Choubert, 1964), which we interpret as the maximum elevation reached by the basin fill before erosion started.

The Moulouya river has a knickzone with a vertical drop of 300 – 400 m located at the boundary between the Arhbalou and Missouri basins. Laville et al. (2007) related this knickzone to active deformation in the Tamdafelt fold system, located just at the base of the knickzone. However, the knickzone as a whole coincides with the contact between the easily erodible sediments of the Missouri basin and Jurassic carbonates/Paleozoic basement rocks. Alternatively, we propose that the knickzone is related to uplift that affected the entire drainage basin, which caused upstream knickpoint propagation until the river lost its erosive capacity at the lithological boundary. The knickzone in the Moulouya river is 150 – 250 m lower than in its tributaries draining the High Plateaus. Within the middle of the Arhbalou basin (upstream of the Moulouya's knickzone), the Gara of Midelt is a 100 m-high butte composed of Neogene sediments, thus providing a minimum estimate of the elevation of the basin fill, and supporting the role of active erosion in landscape evolution.

7.2. Thrust surface uplift of the Jebel Bou Naceur

The main rivers draining the Jebel Bou Naceur to the Missouri and Guercif basins show knickzones with higher difference in elevation than those measured in tributaries draining the High Plateaus. Laville et al. (2007) and Delcaillau et al. (2008) analyzed Quaternary deposits and knickpoints along major streams in the southern flank of the Middle Atlas, and interpreted them as related to recent thrust tectonic deformation, though they did neither quantify deformation rates nor discuss the potential role of regional uplift. The impressive 1000 m-high knickzone

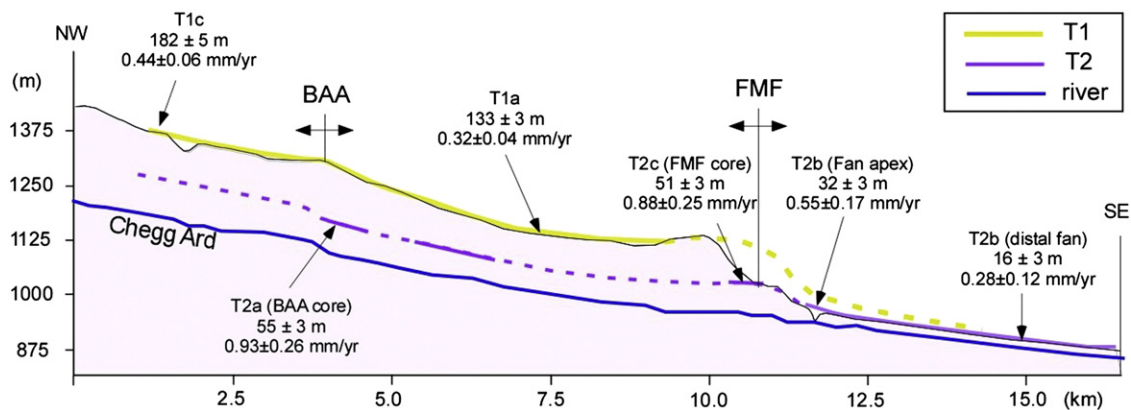


Fig. 9. Topographic profile traced parallel to the Chegg Ard river along its eastern margin (see Fig. 6b for location). Surfaces T1 and T2 are projected in the same plane, in continuous line where preserved, and dashed line were inferred. The figure shows the difference in elevation of terraces T1 and T2 with respect to the active Chegg Ard channel at both sides of the tectonic structures. Incision rates in mm/yr are also shown along the profile.

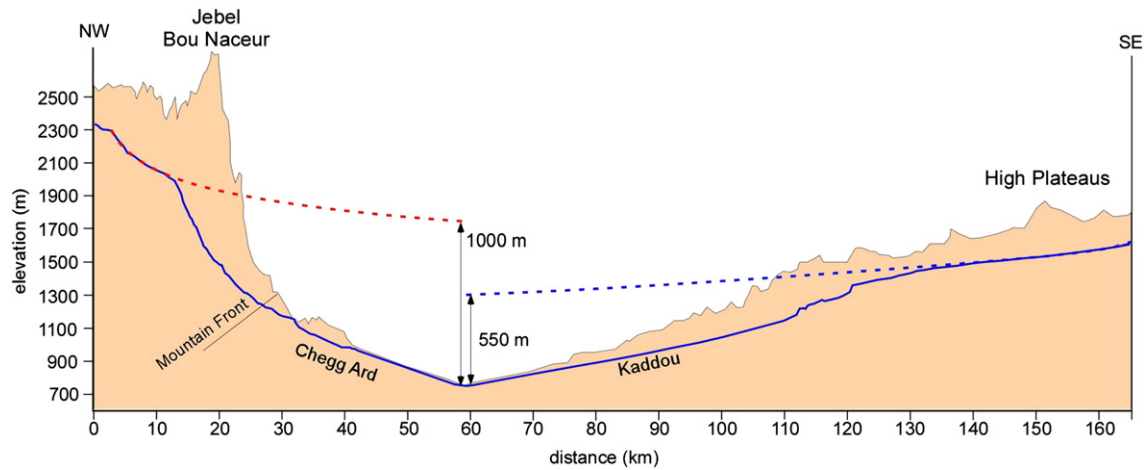


Fig. 10. Topographic profile across the Missouri basin and its margins from the Jebel Bou Naceur to the High Plateaus (see Fig. 3 for location), with the longitudinal profiles of the Chegg Ard and Kaddou rivers projected in the same plane. The knickzone of the Kaddou river is 550 m-high and is related to the regional-scale surface uplift affecting the entire fluvial network. The difference in elevation between the Chegg Ard river and Kaddou river knickzones (450 m) is probably due to local (thrust-related) recent surface uplift of the Jebel Bou Naceur.

of the Chegg Ard river (Fig. 5a) was interpreted exclusively as a result of recent out-of-sequence thrusting by these authors.

The El Mansoor, El Berd and Timrhout tributaries drain the eastern Jebel Bou Naceur to the Guercif basin (Fig. 3) and have 700–800 m-high knickzones (Fig. 5c and d). We propose that in the same way as in tributaries draining the High Plateaus, 500–550 m of the total height of these knickzones is due to regional-scale uplift, whereas the remaining 450–500 m in the central Southern Middle Atlas frontal zone (Fig. 10) and 200–300 m in the eastern edge of the Jebel Bou Naceur can be explained by the localized (thrust-related) uplift of the Middle Atlas associated with its frontal structures. In the Chegg Ard valley, signs of tectonic deformation in Quaternary alluvial deposits attest the active structures emerging within the Missouri basin. Delcaillau et al. (2008) proposed small knickpoints within the Missouri basin and relate them to active structures too. We argue that knickpoint preservation is rare within the basin where streams flow over easily erodible sediments. Instead, knickpoints retreat upstream until they reach more resistant rock types at the basin margin. Resistant rocks are more difficult for the streams to erode, and therefore, knickpoints become knickzones that remain at the lithological boundary for some time, progressively increasing in height. Hence, neither the current location nor the elevation of knickzones along the Moulouya fluvial network can be simply related to active thrust deformation as suggested by Delcaillau et al. (2008).

7.3. Regional (mantle-driven) versus local (thrust-related) surface uplift rates

Our TCN dating of T1 and T2 terraces allows us to calculate incision rates at different points along the Chegg Ard valley. Moreover, the two obtained ages (T2: 62 ± 14 ka and T1: 411 ± 55 ka) enable us to examine incision rates at different time spans, particularly for the area affected by surface uplift due to the FMF. Incision rates measured in the upper Chegg Ard valley must result from combined mantle-driven surface uplift and structural surface uplift produced by the frontal structures of the Middle Atlas, named the FMF and the Beni Aioun anticline, which affect both T1 and T2 surfaces. For the lower reach of the Chegg Ard, downstream from the frontal active structures, we argue that estimated incision rates are rather valid for the Moulouya river, which constitute the base level for the Middle Atlas tributaries. Thus, these rates can be taken as a proxy for the recent surface uplift rates related to dynamic topography within the Moulouya drainage basin, i.e., they represent the large-scale regional surface uplift due to buoyancy changes in the mantle not directly related to crustal tectonic shortening (e.g., Coblenz and Karlstrom, 2011; Nereson et al., 2013 for terminology).

Average regional surface uplift rates since the latest Miocene or earliest Pliocene were estimated in the northern Middle Atlas by Babault et al. (2008) at ~ 0.2 mm yr⁻¹, on the basis of elevated Messinian marine deposits, scarcely eroded and lying at 1200 m.a.s.l. in the Skoura area, only 65 km WNW of our study area. The marine Messinian deposits dated by Krijgsman and Langereis (2000) in the center of the Guercif basin are significantly lower, at 450–650 m.a.s.l., and the resulting surface uplift rate here is of ~ 0.1 mm yr⁻¹. Hence, we retain the value of 0.1–0.2 mm yr⁻¹ based on Messinian shallow marine deposits as an average long-term surface uplift in the study area during the late Pleistocene. The incision rate of 0.28 ± 0.12 mm yr⁻¹ at the distal part of T2b in the Missouri basin is of the same order of magnitude, or slightly greater than this average long-term surface uplift (Babault et al., 2008). Nevertheless, as discussed above, T2-based rates might be slight overestimations of the true values.

We argue that entrenchment of the lower Chegg Ard river since ~ 411 ka is keeping pace with the rising dynamic topography at a rate of ~ 0.1 – 0.2 mm yr⁻¹. Under this assumption, the fluvial incision rate calculated for T1c near the Jebel Bou Naceur mountain front at 0.44 ± 0.06 mm yr⁻¹ (Fig. 9) can be divided into ~ 0.1 – 0.2 mm yr⁻¹ of regional surface uplift plus ~ 0.3 mm yr⁻¹ of thrust-related surface uplift.

The combined geomorphic analysis of river profiles and the incision rates presented above provide inferences on the recent tectonic and erosional history of the Missouri basin. We have showed that the Chegg Ard river profile exhibits a knickpoint with a height of 1000 m, 500–550 m of which might be explained by mantle-driven (regional) surface uplift and the remaining 450–500 m by upthrusting of the Jebel Bou Naceur (Fig. 10). However, our geochronological data suggest that since the Middle Pleistocene the rate of local structural surface uplift has been greater than that of regional surface uplift. Our calculations imply a local structural surface uplift rate of ~ 0.3 mm yr⁻¹ since the Middle Pleistocene within the Missouri basin close to the mountain front in association with the two frontal structures. We cannot discard however the possibility that other active structures are present in the mountain area, but, as a first approximation, we retain the minimum rate of 0.3 mm yr⁻¹, and at such a rate, the 450–500 m height of the knickzone related to thrust activity would have been produced in 1.2–1.5 Ma.

The capture of the Missouri basin generated a knickpoint that propagated upwards along the entire Moulouya catchment until its present-day location at the lithological contrasts along the basin margins. Favoring this view, terrace T1 is the oldest Pleistocene deposit, being characterized by larger clasts that suggest a very high-energy transportational/depositional setting, which, in turn, might be related to the arrival of the knickpoint to the mountain front. The thick alluvial

deposits reported by Bouazza et al. (2009) in the outlet of two gorges incised by the Za and Moulouya rivers in Beni Snassen and Horts Chain may have had a similar origin. Alternatively, the formation of T2 could be climatically controlled, as suggested by Arboleya et al. (2008) for the extensive Quaternary fanglomerates of similar age in the Ouarzazate basin, or due to pulses in the FMF as suggested by Delcaillau et al. (2008).

8. Conclusions

The geomorphic analysis of the Moulouya drainage network within the Missour basin and adjacent highlands (Middle Atlas and High Plateaus) reveals the existence of knickpoints or knickzones along most streams. The knickpoints are located in the rivers draining the tectonically active margin of the Middle Atlas, as well as in those draining the tectonically quiescent High Plateaus. The systematic presence of knickpoints attests adjustment of the fluvial network due to regional (long-wavelength) surface uplift of mantle origin (dynamic topography), which resulted in the Missour basin changing from dominantly aggradational to erosional in the late Pliocene or early Quaternary. Geomorphic evidence shows that the knickpoints related to regional surface uplift propagated upstream along the Moulouya river and its tributaries. The height of knickpoints along the rivers draining the undeformed (High Plateaus) margin indicates that 500–550 m of sediments have been eroded in the central parts of the Neogene Missour and Guercif basins. In contrast, rivers draining the tectonically active margin of the Middle Atlas (Jebel Bou Naceur) show 800–1000 m-high knickpoints. From the undeformed margin, it can be inferred that 500–550 m of this height might be explained by regional dynamic surface uplift, whereas the remaining 450–500 m in the central part of the southern Middle Atlas Front and the 200–300 m in the northeastern edge of the Middle Atlas might be related to thrust uplift of the Jebel Bou Naceur (Fig. 10).

Two Quaternary deformed river terraces in the Chegg Ard valley have been dated at 62 ± 14 ka and 411 ± 55 ka. Dated river terraces allow incision rates to be calculated. This in turn, can be related to the combined surface uplift triggered by both the Middle Atlas structures emerging within the basin, and by large-scale mantle buoyancy since the Middle Pleistocene. Moreover, from terrace deformation we estimate surface uplift along the foreland folds to be $\sim 0.3 \text{ mm yr}^{-1}$. This discriminates localized uplift from the background large-scale surface uplift of $\sim 0.1\text{--}0.2 \text{ mm yr}^{-1}$ in the central part of the Missour basin

Acknowledgments

This research was supported by Spanish projects CGL2010-15416 and CGL2007-66431-CO2-01 (TOPOMED), and Consolider-Ingenio2010 CSD2006-00041 (TOPOIBERIA). Mohammed Charroud is thanked for early guidance to the field area. The comments by J.V. Pérez-Peña, an anonymous reviewer, and the editor A. Azor helped substantially to improve the original manuscript.

References

- Anahnah, F., Galindo-Zaldívar, J., Chalouan, A., Pedrera, A., Ruano, P., Pous, J., Heise, W., Ruiz-Constan, A., Benmakhlouf, M., Lopez-Garrido, A.C., Ahmamou, M., Sanz de Galdeano, C., Arzate, J., Ibarra, P., Gonzalez-Castillo, L., Bouregba, N., Corbo, F., Asensio, E., 2011. Deep resistivity cross section of the intraplate Atlas Mountains (NW Africa): new evidence of anomalous mantle and related Quaternary volcanism. *Tectonics* 30, 1–9.
- Anderson, R.S., Repka, J.L., Dick, G.S., 1996. Explicit treatment of inheritance in dating depositional surfaces using in situ ^{10}Be and ^{26}Al . *Geology* 24, 47–51.
- Arboleya, M.L., Teixell, A., Charroud, M., Julivert, M., 2004. A structural transect through the High and Middle Atlas of Morocco. *J. Afr. Earth Sci.* 39, 319–327.
- Arboleya, M.-L., Babault, J., Owen, L.A., Teixell, A., Finkel, R.C., 2008. Timing and nature of fluvial incision in the Ouarzazate foreland basin, Morocco. *J. Geol. Soc. Lond.* 165, 1059–1073.
- Ayarza, P., Carbonell, R., Teixell, A., Palomeras, I., Martí, D., Kchikach, M., Levander, A., Gallart, J., Arboleya, M.L., Alcalde, J., Fernández, M., Charroud, M., Amrhar, M., 2014. Crustal thickness and velocity structure across the Moroccan Atlas from long offset wide-angle reflection seismic data: the SIMA experiment. *Geochem. Geophys. Geosyst.* 15, 1698–1717.
- Babault, J., Teixell, A., Arboleya, M.L., Charroud, M., 2008. A Late Cenozoic age for long-wavelength surface uplift of the Atlas Mountains of Morocco. *Terra Nova* 20, 102–107.
- Balco, G., Stone, J.O., Lifton, N.A., Dunai, T.J., 2008. A complete and easily accessible means of calculating surface exposure ages or erosion rates from ^{10}Be and ^{26}Al measurements. *Quat. Geochronol.* 8, 174–195.
- Barbero, L., Jabaloy, A., Gómez-Ortiz, D., Pérez-Peña, J.V., Rodríguez-Peces, M.J., Tejero, R., Estupiñán, J., Azdimousa, A., Vázquez, M., Asebriy, L., 2011. Evidence for surface uplift of the Atlas Mountains and the surrounding peripheral plateaux: combining apatite fission track results and geomorphic indicators in the Western Moroccan Meseta (Coastal Variscan Paleozoic Basement). *Tectonophysics* 502, 90–104.
- Barcos, L., Jabaloy, A., Azdimousa, A., Asebriy, L., Gómez-Ortiz, D., Rodríguez-Peces, M.J., Tejero, R., Pérez-Peña, J.V., 2014. Study of relief changes related to active doming in the eastern Moroccan Rif (Morocco) using geomorphological indices. *J. Afr. Earth Sci.* 100, 493–509.
- Beauchamp, W., Barazangi, M., Demnati, A., El Alji, M., 1996. Intracontinental rifting and inversion: Missour Basin and Atlas Mountains, Morocco. *AAPG Bull.* 80, 1459–1482.
- Begin, Z.B., Meyer, D.F., Schumm, S.A., 1981. Development of longitudinal profiles of alluvial channels in response to base-level lowering. *Earth Surf. Process. Landf.* 6, 49–68.
- Benda, L., Dunne, T., 1997. Stochastic forcing of sediment routing and storage in channel networks. *Water Resour. Res.* 33, 2865–2880.
- Bernini, M., Boccaletti, M., Gelatti, R., Moratti, G., Papani, G., El Mokhtari, J., 1999. Tectonics and sedimentation in the Taza-Guercif basin, northern Morocco: implications for the Neogene evolution of the Rif-Middle Atlas orogenic system. *J. Pet. Geol.* 22, 115–128.
- Bernini, M., Boccaletti, M., Moratti, G., Papani, G., 2000. Structural development of the Taza-Guercif Basin as a constraint for the Middle Atlas Shear Zone tectonic evolution. *Mar. Pet. Geol.* 17, 391–408.
- Bishop, P., 2007. Long-term landscape evolution: linking tectonics and surface processes. *Earth Surf. Process. Landf.* 32, 329–365.
- Bishop, P., Hoey, T.B., Jansen, J.D., Artza, L.L., 2005. Knickpoint recession rate and catchment area: the case of uplifted rivers in Eastern Scotland. *Earth Surf. Process. Landf.* 30, 767–778.
- Bouazza, A., AïtBrahim, L., Dugué, O., Laville, E., Delcaillau, B., Cattaneo, G., Charroud, M., de Luca, P., 2009. Changements Sédimentaires dans les Bassins Néogènes de Taurirt et Guercif (Maroc Oriental): Recherche de l'épisode d'érosion Messinienne. *Eur. J. Sci. Res.* 28, 317–327.
- Boulton, S.J., Stokes, M., Mather, A.E., 2014. Transient fluvial incision as an indicator of active faulting and Plio-Quaternary uplift of the Moroccan High Atlas. *Tectonophysics* 633, 16–33.
- Burbank, D.W., Anderson, R.S., 2001. *Tectonic Geomorphology*. Blackwell Science, Malden (274 pp.).
- Burbank, D.W., Leland, J., Fielding, E., Anderson, R.S., Brozovic, N., Reid, M.R., Duncan, C., 1996. Bedrock incision, rock uplift and threshold hillslopes in the northwestern Himalaya. *Nature* 379, 505–510.
- Charroud, A., 2002. Evolution géodynamique des hauts plateaux (Maroc) et de leurs bordures du Mésozoïque au Cénozoïque (Thèse 3è Cycle), Université Sidi Mohamed Ben Abdellah, Fes (314 pp.).
- Choubert, A., 1964. Carte géologique du Maroc, sheet NI-30-IX-2: Hassi el Ahmar. Service Géologique du Maroc, Notes et Mémoires. Ministère de l'Énergie et des Mines, Direction de la Géologie, Rabat.
- Coblentz, D., Karlstrom, K.E., 2011. Tectonic geomorphometrics of the western United States: speculations on the surface expression of upper mantle processes. *Geochem. Geophys. Geosyst.* 12, Q11002. <http://dx.doi.org/10.1029/2011GC003579>.
- Crosby, B.T., Whipple, K.X., 2006. Knickpoint initiation and distribution within fluvial networks: 236 waterfalls in the Waipaoa River, North Island, New Zealand. *Geomorphology* 82 (1–2), 16–38.
- Delcaillau, B., Laville, E., Carozza, J.-M., Dugué, O., Charroud, M., Amrhar, M., 2008. Morphotectonic evolution of the Jebel Bou Naceur in the South Middle Atlas Fault Zone (Morocco). *Compt. Rendus Geosci.* 339, 553–561.
- Desilets, D., Zreda, M., 2003. Spatial and temporal distribution of secondary cosmic-ray nucleon intensities and applications to in-situ cosmogenic dating. *Earth Planet. Sci. Lett.* 206, 21–42.
- Desilets, D., Zreda, M., Prabu, T., 2006. Extended scaling factors for in situ cosmogenic nucleides: new measurements at low latitude. *Earth Planet. Sci. Lett.* 246, 265–276.
- Dutour, A., 1983. Etude géomorphologique de la partie occidentale de la Haute Moulouya (Maroc) (Thèse 3è Cycle), Poitiers (361 pp.).
- Dunai, T., 2001. Influence of secular variation of the magnetic field on production rates of in situ produced cosmogenic nuclides. *Earth Planet. Sci. Lett.* 193, 197–212.
- Ellouz, N., Patriat, M., Gaulier, J.-M., Bouatmani, R., Sabounji, S., 2003. From rifting to Alpine inversion: Mesozoic and Cenozoic subsidence history of some Moroccan basins. *Sediment. Geol.* 156, 185–212.
- Flint, J.J., 1974. Stream gradient as a function of order, magnitude, and discharge. *Water Resour. Res.* 10 (5), 969–973.
- Fuller, J., Fernández, M., Afonso, J.C., Vergés, J., Zeyen, H., 2010. The structure and evolution of the lithosphere–asthenosphere boundary beneath the Atlantic–Mediterranean Transition Region. *Lithos* 120, 74–95.
- García, A.F., 2006. Thresholds of strath genesis deduced from a landscape response to stream piracy by Pancho Rico Creek in the Coast Ranges of central California. *Am. J. Sci.* 306, 655–681.
- Gile, L.H., Hawley, J.W., Grossman, R.B., 1981. Soils and geomorphology in the Basin and Range area of southern New Mexico — guidebook to the Desert Project. *New Mex. Bur. Min. Mineral Resour. Mem.* 39 (222 pp.).

- Gorokhovich, Y., Voustianiouk, A., 2006. Accuracy assessment of the processed SRTM-based elevation data by CGIAR using field data from USA and Thailand and its relation to the terrain characteristics. *Remote Sens. Environ.* 104, 409–415.
- Goldrick, G., Bishop, P., 2007. Regional analysis of bedrock stream long profiles: evaluation of Hack's SL form, and formulation and assessment of an alternative (the DS form). *Earth Surf. Process. Landf.* 32, 649–671.
- Gomez, F., Allmendinger, R., Barazangi, M., Er-Raji, A., Dahmani, M., 1998. Crustal shortening and vertical strain partitioning in the Middle Atlas mountains of Morocco. *Tectonics* 17, 520–533.
- Gomez, F., Barazangi, M., Demnati, A., 2000. Structure and evolution of the Neogene Guercif Basin at the junction of the Middle Atlas Mountains and the Rif Thrust Belt, Morocco. *AAPG Bull.* 84, 1340–1364.
- Hack, J.T., 1957. Studies of longitudinal stream profiles in Virginia and Maryland. *U. S. Geol. Surv. Prof. Pap.* 294 (B), 45–94.
- Hancock, G.S., Anderson, R.S., Chadwick, O.A., Finkel, R.C., 1999. Dating fluvial terraces with ^{10}Be and ^{26}Al profiles: application to the Wind River, Wyoming. *Geomorphology* 27, 41–60.
- Hoke, G.D., Isacks, B.L., Jordan, T.E., Blanco, N., Tomlinson, A.J., Ramezani, J., 2007. Geomorphic evidence for post-10 Ma uplift of the western flank of the central Andes. *Tectonics* 26. <http://dx.doi.org/10.1029/2006TC002082>.
- Howard, A.D., Kerby, G., 1983. Channel changes in badlands. *Geol. Soc. Am. Bull.* 94 (6), 739–752.
- Kohl, C.P., Nishiizumi, K., 1992. Chemical isolation of quartz for measurement of in situ-produced cosmogenic nuclides. *Geochim. Cosmochim. Acta* 56, 3583–3587.
- Korup, O., 2006. Rock-slope failure and the river long profile. *Geology* 34, 45–48.
- Krijgsman, W., Langereis, C.G., 2000. Magnetostratigraphy of the Zobzit and Koudiat Zarga sections (Taza-Guercif Basin, Morocco): implications for the evolution of the Rifian Corridor. *Mar. Pet. Geol.* 17, 359–371.
- Krijgsman, W., Langereis, C.G., Zachariasse, W.J., Boccaletti, M., Moratti, G., Gelati, R., Iaccarino, S., Papani, G., Villa, G., 1999. Late Neogene evolution of the Taza-Guercif Basin (Rifian Corridor, Morocco) and implications for the Messinian salinity crisis. *Mar. Geol.* 153, 147–160.
- Lal, D., 1991. Cosmic ray labeling of erosion surfaces: in situ nuclide production rates and erosion models. *Earth Planet. Sci. Lett.* 104, 429–439.
- Lancaster, S.T., Grant, G.E., 2006. Debris dams and the relief of headwater streams. *Geomorphology* 82, 84–97.
- Lavé, J., Avouac, J.P., 2001. Fluvial incision and tectonic uplift across the Himalayas of central Nepal. *J. Geophys. Res.* 106, 26561–26591.
- Laville, E., Delcaillau, B., Charrout, M., Dugué, O., AitBrahim, L., Cattaneo, G., Deluca, P., Bouazza, A., 2007. The Plio-Pleistocene evolution of the Southern Middle Atlas Fault Zone (SMAFZ) front of Morocco. *Int. J. Earth Sci.* 96, 497–515.
- Lifton, N., Bieber, J., Clem, J., Duldig, M., Evenson, P., Humble, J., Pyle, R., 2005. Addressing solar modulation and long-term uncertainties in scaling secondary cosmic rays for in situ cosmogenic nuclide applications. *Earth Planet. Sci. Lett.* 239, 140–161.
- Matmon, A., Simhai, O., Amit, R., Haviv, I., Porat, N., McDonald, E., Benedetti, L., Finkel, R., 2009. Desert pavement-coated surfaces in extreme desert presents the longest-lived landforms on Earth. *Geol. Soc. Am. Bull.* 121, 688–697.
- Miller, M.S., Becker, T.W., 2014. Reactivated lithospheric-scale discontinuities localize dynamic uplift of the Moroccan Atlas Mountains. *Geology* 42, 35–38.
- Nereson, A., Stroud, J., Karlstrom, K., Heizler, M., McIntosh, W., 2013. Dynamic topography of the western Great Plains: geomorphic and $^{40}\text{Ar}/^{39}\text{Ar}$ evidence for mantle-driven uplift associated with the Jemez lineament of NE New Mexico and SE Colorado. *Geosphere* 9, 521–545.
- Nishiizumi, K., Imamura, M., Caffee, M.W., Southon, J.R., Finkel, R.C., McAninch, J., 2007. Absolute calibration of Be-10 AMS standards. *Nuclear Instruments and Methods in Physics Research. Section B: Beam Interactions with Materials and Atoms* 258, 403–413.
- Palomeras, I., Thurner, S., Levander, A., Liu, K., Villaseñor, A., Carbonell, R., Harnafi, M., 2014. Finite-frequency Rayleigh wave tomography of the western Mediterranean: mapping its lithospheric structure. *Geochem. Geophys. Geosyst.* 15, 140–160.
- Pastor, A., Teixell, A., Arboleya, M.L., 2012. Rates of Quaternary deformation in the Ouarzazate Basin (Southern Atlas Front, Morocco). *Ann. Geophys.* 55, 1003–1016.
- Paul, J., Roberts, G., White, N., 2014. The African landscape through space and time. *Tectonics* 33, 898–935.
- Portenga, E.W., Bierman, P.R., 2011. Understanding Earth's eroding surface with ^{10}Be . *Geol. Today* 21, 4–10.
- Pigati, J.S., Lifton, N.A., 2004. Geomagnetic effects on time-integrated cosmogenic nuclide production with emphasis on in situ ^{14}C and ^{10}Be . *Earth Planet. Sci. Lett.* 226, 193–205.
- Quezada, J., Cerda, J.L., Jensen, A., 2010. Efectos de la tectónica y el clima en la configuración morfológica del relieve costero del norte de Chile. *Andean Geol.* 37, 78–109.
- Sani, F., Zizi, M., Bally, A.W., 2000. The Neogene–Quaternary evolution of the Guercif Basin (Morocco) reconstructed from seismic line interpretation. *Mar. Pet. Geol.* 17, 343–357.
- Schildgen, T.F., Cosentino, D., Bookhagen, B., Niedermann, S., Yildırım, C., Echter, H., Wittmann, H., Strecker, M.R., 2012. Multi-phased uplift of the southern margin of the Central Anatolian Plateau, Turkey: a record of tectonic and upper mantle processes. *Earth Planet. Sci. Lett.* 317–318, 85–95.
- Sébrier, M., Siame, L., Zouine, E.M., Winter, T., Missenard, Y., Leturmy, P., 2006. Active tectonics in the Moroccan High Atlas. *Compt. Rendus Geosci.* 338, 65–79.
- Snyder, N.P., Whipple, K.X., Tucker, G.E., Merritts, D.J., 2002. Interactions between onshore bedrock-channel incision and nearshore wave-base erosion forced by eustasy and tectonics. *Basin Res.* 14, 105–127.
- Staiger, J., Gosse, J., Toracinta, R., Oglesby, B., Fastook, J., Johnson, J.V., 2007. Atmospheric scaling of cosmogenic nuclide production: climate effect. *J. Geophys. Res.* 112, B02205.
- Stone, J.O., 2000. Air pressure and cosmogenic isotope production. *J. Geophys. Res.* 105, 23753–23759.
- Sun, D., Miller, M.S., Holt, A.F., Becker, T.W., 2014. Hot upwelling conduit beneath the Atlas Mountains, Morocco. *Geophys. Res. Lett.* 41, 8037–8044.
- Teixell, A., Arboleya, M.L., Julivert, M., Charrout, M., 2003. Tectonic shortening and topography in the central High Atlas (Morocco). *Tectonics* 22. <http://dx.doi.org/10.1029/2002TC001460>.
- Teixell, A., Ayarza, P., Zeyen, H., Fernandez, M., Arboleya, M.L., 2005. Effects of mantle upwelling in a compressional setting: the Atlas Mountains of Morocco. *Terra Nova* 17, 456–461.
- Whipple, K.X., 2001. Fluvial landscape response time: how plausible is steady-state denudation? *Am. J. Sci.* 301, 313–325.
- Whipple, K.X., Tucker, G.E., 1999. Dynamics of the stream-power river incision model: implications for height limits of mountain ranges, landscape response timescales, and research needs. *J. Geophys. Res.* 104 (B8), 17,661–17,674.
- Wobus, C., Whipple, K.X., Kirby, E., Snyder, N., Johnson, J., Spyropolou, K., Crosby, B., Sheehan, D., 2006. Tectonics from topography: procedures, promise, and pitfalls. *Geol. Soc. Am. Spec. Pap.* 398, 55–74.
- Zeyen, H., Ayarza, P., Fernández, M., Rimi, A., 2005. Lithospheric structure under the western African–European plate boundary: a transect across the Atlas Mountains and the Gulf of Cadiz. *Tectonics* 24. <http://dx.doi.org/10.1029/2004TC001639>.